TECHNOLOGICAL LIMITATIONS OF MONOLITHIC HIGH-FREQUENCY OSCILLATORS IN MOS AND BIPOLAR PROCESSES

Sreenath Thoka, Chao Su and Randall Geiger

Department of Electrical and Computer Engineering
Iowa State University, Ames, IA 50011, U.S.A.
Email: sreenat, schao, rlgeiger@iastate.edu

ABSTRACT

The relationship between the maximum oscillation frequency and the process parameter f_T for two useful classes of oscillators is developed. Results show that the oscillation frequency of a class of LC-tank oscillators can be substantially higher than f_T if high-Q inductors are used

1. INTRODUCTION

It is well recognized that the design of high frequency oscillators becomes increasingly challenging as the oscillation frequency approaches the f_T of a process [1]. Conventional wisdom suggests that the maximum frequency of operation of circuits must be substantially lower than the f_T of the transistors used in the circuit. Clock and Data recovery circuits operating at 40 GHz and above have been reported [2,3] using SiGe processes with f_T in the range of 70 GHz. Quadrature ring oscillators have been reported [4] with operating frequencies of up to $0.7f_T$ of the process. With increasing opportunities in the serial communications space for circuits with oscillators operating in the 20GHz and 40GHz frequency ranges, frequencies which are close to or beyond the f_T of transistors in state of the art processes, the question of what is the maximum frequency of operation of circuits in general and oscillators in particular naturally arises.

In this work, the fundamental limit on oscillation frequency of voltage controlled oscillators (VCOs) with respect to f_T is investigated.. In the following section , notation for standard models for non-ideal inductors is established. In subsequent sections, the maximum frequency of operation relative to the f_T of the process for a class of LC-tank oscillators (alternatively termed negative resistance LC oscillators) and ring oscillators is developed.

2. MODEL OF NON-IDEAL INDUCTOR

Two approximate but widely used models for a non-ideal inductor are shown in Fig. 1. If the inductor L with series resistance R_s is operating in a circuit at or near a frequency ω_x, its Q factor is defined by the expression:

$$Q = \frac{\omega_x L}{R_s} \tag{1}$$

At frequencies around ω_x, the inductor can be equivalently modeled by the parallel circuit on the right where the conductance G_p relates to the resistance R_s as

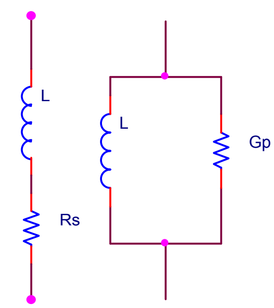

Figure 1. Two Equivalent Models for a Non-ideal Inductor

$$G_p = \frac{1}{Q^2 R_s} \tag{2}$$

It follows from (1) and (2) that the Q of the inductor can be expressed in terms of G_p as:

$$Q = \frac{1}{\omega_x L G_p} \tag{3}$$

3. NEGATIVE RESISTANCE LC OSCILLATORS

Two variants of a negative resistance LC oscillator are shown in Fig. 2. These basic structures are widely used as integrated LC Voltage Controlled Oscillators (VCO) that operate at frequencies in the 5 GHz to 10GHz range. The cross-coupled pair of active devices provides the negative resistance needed to sustain oscillation. The active device is typically either a MOSFET or a BJT. Both circuits have identical small-signal half circuits that can be used to obtain the oscillation criterion and the oscillation frequency.

The half-circuit for these oscillators is shown in Fig. 3. In this small signal half-circuit, L is the inductance, the G and C include any parasitics of the small-signal transistor model along with the finite output impedance, and the active device is assumed to be a transistor that can be modeled as an ideal transconductance amplifier with gain g_m.

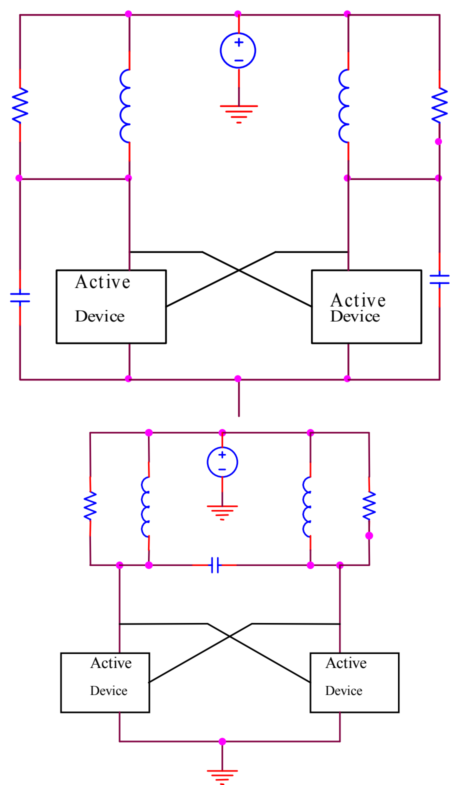

Figure 2. Negative Resistance Oscillator Topologies

G (for the parallel inductor model) and C for the MOSFET and BJT are given respectively by the equations:

MOSFET:

$$G = G_p + g_o \tag{4}$$

$$C = C_L + C_{gs} \tag{5}$$

BJT:

$$G = G_p + g_o + g_\pi \tag{6}$$

$$C = C_L + C_\pi \tag{7}$$

where g_o is the output conductance of the transistor, C_L is the total load capacitance seen at the output node of the transistor, C_π (C_{gs}) is the base-emitter (gate-source) input capacitance of the BJT (MOSFET) transistor and g_π (0) is the small signal input conductance of the BJT (MOSFET).

It follows from a simple analysis that the characteristic polynomial of these oscillators is given by

$$D(s) = s^2 + s\frac{G - g_m}{C} + \frac{1}{LC} \tag{8}$$

It thus follows from (8) that the oscillation criterion is

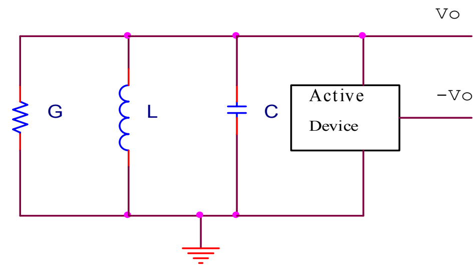

Figure 3. Half-circuit for Oscillators shown in Fig. 2:

$$g_m \geq G \tag{9}$$

and the frequency of oscillation (when g_m=G) is

$$\omega_{OSC} = \frac{1}{\sqrt{LC}} \tag{10}$$

It should be emphasized that the expression for the oscillation frequency is only valid when the inequality in (9) becomes an equality. As the poles move farther into the right half-plane for larger values of g_m, the circuit behaves nonlinearly and the oscillation frequency will decrease.

If we substitute the model parameters from (4), (5), (6) and (7) into (9) and (10), it follows that the oscillation criterion and oscillation frequency of the oscillator become

MOSFET:

$$g_m \geq G_p + g_o \tag{11}$$

$$\omega_{OSC} = \frac{1}{\sqrt{L(C_L + C_{gs})}} \tag{12}$$

BJT:

$$g_m \geq G_p + g_o + g_\pi \tag{13}$$

$$\omega_{OSC} = \frac{1}{\sqrt{L(C_L + C_\pi)}} \tag{14}$$

It is known that the parameter f_T or ω_T for the MOSFET (BJT) is defined to be the frequency where the short-circuit common-source (common-emitter) current gain drops to unity. It can be shown that ω_T is approximately given by the expressions:

MOSFET:

$$\omega_T = \frac{g_m}{C_{gs}} \tag{15}$$

BJT:

$$\omega_T = \frac{g_m}{C_\pi} \tag{16}$$

The maximum frequency of operation is not apparent from (15) and (16).

MOSFET:

We now substitute the inductor Q and ω_T expressions from (3) and (15) into (12) to obtain

$$\omega_{OSC} = \sqrt{\omega_x}\sqrt{Q\omega_T \frac{(g_m - g_o)}{g_m + C_L\omega_T}} \qquad (17)$$

If it is now assumed that the inductor Q is characterized at the oscillation frequency, then $\omega_x = \omega_{OSC}$, so (17) reduces to

$$\omega_{OSC} = Q\omega_T \frac{(g_m - g_o)}{g_m + C_L\omega_T} \qquad (18)$$

Although there is still an ω_T dependence on g_m, (18) can be maximized. If C_L can be set to zero and since g_m is made large, it follows that the maximum frequency of oscillation is given by

$$\omega_{OSC-MAX} \cong Q\omega_T \qquad (19)$$

From this expression, it is apparent that the frequency of oscillation can be considerably higher than the ω_T of a process for even modestly high-Q inductors. This is not particularly surprising since the transistor needs to only provide a modest correction for the loss of the inductor to make the circuit oscillate.

BJT:

The major difference in the BJT and MOSFET circuits is the presence of the parameter g_π in the BJT model. However, at high frequencies, the reactive admittance of the capacitor C_π is much larger than g_π so one would expect (19) to apply for the BJT as well. This is indeed the case. Substituting the inductor Q and ω_T expressions from (3) and (16) into (14), it follows that the BJT counterparts of (17) and (19) are respectively

$$\omega_{OSC} = \sqrt{\omega_x}\sqrt{Q\omega_T \frac{(g_m - g_o - g_\pi)}{g_m + C_L\omega_T}} \qquad (20)$$

$$\omega_{OSC} = Q\omega_T \frac{(g_m - g_o - g_\pi)}{g_m + C_L\omega_T} \qquad (21)$$

Maximizing (21), it follows that

$$\omega_{OSC-MAX} \cong Q\omega_T \qquad (22)$$

It should be observed from (19) and (22) that, counter to conventional wisdom, the maximum frequency of oscillation is not limited by the ω_T of the process. Although the frequency of oscillation predicted by these equations may not be attainable for other reasons such as a non-ideal inductance, possibly the base-spreading resistance (BJT) or interconnect parasitics simulation results suggest that oscillation at frequencies somewhat above the ω_T of the process is achievable. The effects of velocity saturation in MOSFETs should also be considered although the major implications will likely be captured in the derivation of the expression for ω_T as well.

4. RING OSCILLATORS

An n-stage ring oscillator is shown in Fig. 4, where ideally all of the gain stages have the same gain,

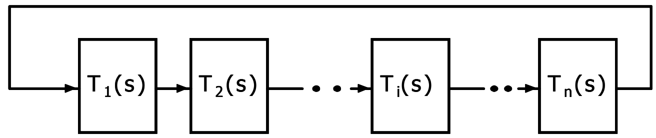

Figure 4. n-Stage Ring Oscillator

$$T_i(s) = T(s) \qquad (23)$$

If each of the gain (delay) stages are realized with the basic amplifiers shown in Fig. 5, the model of each stage is given by

$$T(s) = \frac{-g_m}{sC + g} \qquad (24)$$

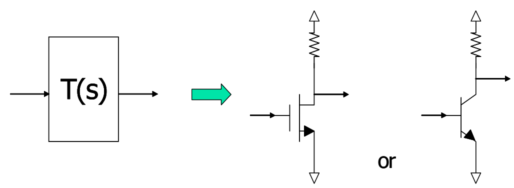

Figure 5 Basic Delay Stages for Ring Oscillator

If a small signal model is used for each active device and if the elements in the overall ring oscillator are regrouped, the equivalent model of each stage shown in Fig. 6 is obtained where

$$g = g_{OUT} + g_{IN} \qquad (25)$$

$$C = C_L + C_{IN} \qquad (26)$$

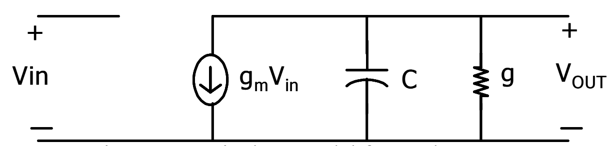

Figure 6. Equivalent Model for Each Stage

It follows from a routine analysis that the loop gain of the ring oscillator is given by the expression

$$LG(s) = T(s)^n \qquad (27)$$

and thus the characteristic polynomial of the ring oscillator obtained by setting *1 – LG(s) = 0* is given by

$$D(s) = (sC + g)^n + g_m^n \qquad (28)$$

It can be readily shown that the poles of the ring oscillator, which are the roots of D(s) lie on a circle in the s-plane of radius ω_o and center ω_c given by

$$\omega_O = \frac{g_m}{C} \quad (29)$$

$$\omega_{\cdot C} = \frac{-g}{C} \quad (30)$$

If there are no losses in the network, T(s) becomes an ideal integrator with $g = 0$ and the pole locus is centered at the origin. Losses in the network move the circle to the left with the center as indicated by (30).

Consider now a case where n = 3, i.e. a three-stage ring oscillator. The pole locations of the three-stage ring oscillator are depicted in Fig. 7.

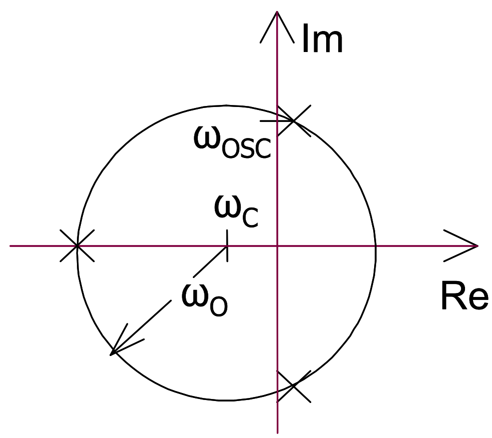

Figure 7. Pole Locations of a Three-Stage Ring Oscillator

The complex conjugate pole-pair in the right half-plane will determine the frequency of oscillation. At the onset of oscillation, it can be shown that the frequency of oscillation is equal to the magnitude of the complex component of the poles as depicted by the frequency ω_{OSC} in Fig. 7. It is easy to show that ω_{OSC} is independent of the losses and is given by the expression

$$\omega_{OSC} = \omega_O \cos 30^0 = 0.87\omega_O \quad (31)$$

If the loss is adjusted by increasing g_m until the pole-pair lies just inside the RHP, the frequency of oscillation given by (31) will be sustained. If the losses are less, the poles will be further in the RHP causing increased distortion of the output waveform and a decrease in the frequency of oscillation. It can be readily shown that the oscillation criterion for the 3-stage ring oscillator is

$$g_m \geq 2g \quad (32)$$

The oscillation criterion is readily satisfied and additional loss must be added if the frequency is to be maximized. Setting C_L to zero, it follows from (15), (16) and (29) that

$$\omega_{O-MAX} = \frac{g_m}{C_{IN}} = \omega_T \quad (33)$$

and hence from (31)

$$\omega_{OSC-MAX} = 0.87\omega_T \quad (34)$$

In contrast to the negative resistance LC oscillator where the frequency of oscillation can exceed ω_T, the oscillation frequency of the basic 3-stage ring oscillator comprised of only active devices is always less than ω_T. It is easy to show that ideally a two–stage ring oscillator has a maximum oscillation frequency of ω_T and that ring oscillators with more than 3 stages will have a maximum frequency of oscillation that is lower than that given by (34).

It should be emphasized however that it is premature to conclude that the ring oscillator structure inherently has an oscillation frequency that is bounded above by ω_T. It is conjectured that if the ring oscillator stage is modified by the inclusion of an inductive element, then the frequency of oscillation of the ring oscillator can also be increased above ω_T of the process. It is also conjectured that such a modification will be easy to implement.

5. CONCLUSION

The maximum oscillation frequencies of an LC-tank oscillator and a basic ring oscillator were introduced. It was shown that the maximum frequency of oscillation of the LC-tank oscillator can be substantially higher than f_T if high-Q inductors are used in the tank whereas that of the basic ring oscillator is bounded from above by f_T.

6. REFERENCES

[1] Rein H.-M. and Moller M. "Design Considerations for Very-High-Speed Si-Bipolar IC's Operating up to 50Gb/s". IEEE JSSC, vol. 31, no. 8, pp. 1076-1090, Aug. 1996.

[2] van der Tang J.D., Kasperkovitz D. and van Roermund A. "A 9.8-11.5-GHz quadrature ring oscillator for optical receivers". IEEE JSSC, vol. 37, no. 3, pp. 438-442, March 2002.

[3] Reinhold M., Dorschky C., Rose E., Pullela R., Mayer P., Kunz F., Baeyens Y., Link T. and Mattina J.-P. "A Fully Integrated 40-Gb/s Clock and Data Recovery IC with 1:4 DEMUX in SiGe Technology". IEEE JSSC, vol. 36, no. 12, pp. 1937-1945, Dec. 2001

[4] Soyuer M. and Warnock J.D. "Multigigahertz Voltage-Controlled Oscillators in Advanced Silicon Bipolar Technology". IEEE JSSC, vol. 27, no. 4, pp. 668 – 670, April 1992.